New Allosteric Modulators of Metabotropic Glutamate Receptor 5 (mGluR5) Found by Ligand-Based Virtual Screening

Steffen Renner,[a] Tobias Noeske,[b] Christopher G. Parsons,[b] Petra Schneider,[c] Tanja Weil,[b] and Gisbert Schneider*[a]

Glutamate is the major excitatory neurotransmitter in the mammalian central nervous system. Its long-term modulating affect on synaptic transmission is mediated by the metabotropic glutamate receptors (mGluR),[1] a family of class III G protein-coupled receptor (GPCR) proteins. This class of GPCRs is characterized by the typical seven transmembrane domain and an additional large extracellular ligand-binding domain.[2] Allosteric modulators that bind to the receptor within the seven transmembrane helix region—that is, the region where the ligand-binding pocket is located in type I and type II GPCRs—represent an attractive class of molecules for addressing several neural disorders associated with mGluR activity.[2] The first selective allosteric antagonists for mGluR5, SIB-1751 (**1**) and SIB-1893 (**2**), were published in 1999 (Scheme 1).[3] SIB-1751 was identified by high-throughput screening (HTS), and SIB-1893 resulted from a UNITY search for analogues.[3] In phosphoinositol (PI) hydrolysis assays, the two molecules revealed IC_{50} values of 3.1 and 2.3 μM, respectively. Chemical variation of SIB-1893 resulted in the much more potent, highly selective mGluR5 antagonist 2-methyl-6-(phenylethynyl)pyridine (MPEP, **3**), which had an IC_{50} of 36 nM in PI hydrolysis assays.[4] Several MPEP analogues (**4**–**9**)[5] with reported low nanomolar activity have been published in the scientific and patent literature since then. Nonetheless, the mode of action of these ligands is not completely understood. Recent publications of MPEP and MPEP derivatives also reported off-target activity[5] and a short plasma half life.[6] In particular, the latter could be attributed to potential metabolic instability of the ethynyl linker.

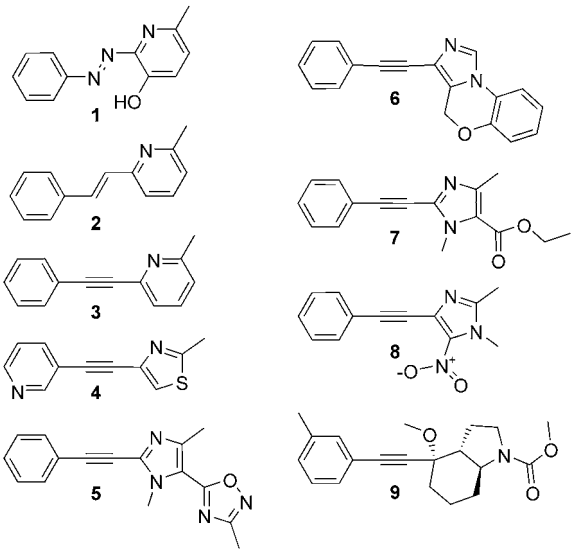

Scheme 1. *Reference allosteric mGluR5 antagonists.*

Pharmacophore-based similarity searching has been proven to be suited to finding new ligands that exhibit similar biological activity but are based on a different chemical scaffold.[7] Using a set of known specific allosteric antagonists of mGluR5 (**3**–**9**),[4,5] which were compiled from scientific and patent literature, we applied a hierarchical, ligand-based virtual-screening approach to identify novel compounds that modulate mGluR5. First, a "drug-likeness" estimation by an artificial neural-network system was employed to prescreen just for molecules with a predicted "drug-like" structure.[8] For subsequent similarity searching, we used the CATS3D descriptor, a 3D extension of the original topology-based CATS approach, both of which were designed for the sake of "scaffold-hopping".[9,10]

CATS3D encodes the conformation of a molecule in the form of a histogram that contains the normalized frequencies of all pairs of atoms of a molecule.[10] Atom pairs were subdivided into groups that were characterized by atom–atom distance ranges in Euclidean space and six different pharmacophore types. 20 equal-distance bins from 0–20 Å were used. One of the pharmacophore types—cation, anion, hydrogen-bond acceptor, hydrogen-bond donor, polar (hydrogen-bond acceptor and hydrogen-bond donor) or hydrophobic—was assigned to each atom by using the ph4_aType function of MOE (Chemical Computing Group Inc., Montréal, Canada; URL: http://www.chemcomp.com). The CATS3D representation is rotation- and translation-invariant, and therefore enables rapid pair-wise comparisons of molecules without the need to explicitly align the molecules.

To form a hypothesis about receptor-bound 3D conformations of **3**–**9**, we used the flexible-alignment tool of MOE. Ligands were successively aligned from **3** to **9** (Figure 1), and

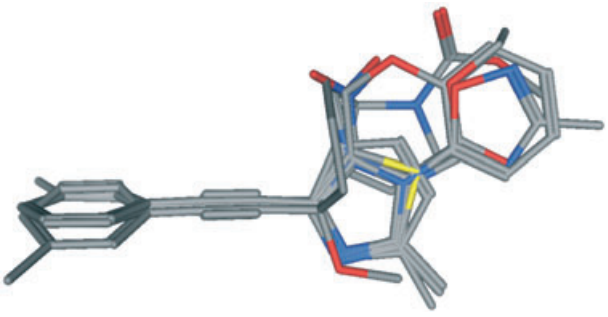

Figure 1. *Flexible pharmacophore-based alignment of reference molecules* ***3***–***9****.*[4,5] *Red: oxygen; blue: nitrogen; yellow: sulfur; gray: carbon.*

[a] *S. Renner, Prof. Dr. G. Schneider*
Johann Wolfgang Goethe-Universität
Institut für Organische Chemie und Chemische Biologie
Marie-Curie-Straße 11, 60439 Frankfurt am Main (Germany)
Fax: (+49) 69-798-29826
E-mail: g.schneider@chemie.uni-frankfurt.de

[b] *T. Noeske, Dr. C. G. Parsons, Dr. T. Weil*
Merz Pharmaceuticals GmbH
Eckenheimer Landstraße 100, 60318 Frankfurt am Main (Germany)

[c] *Dr. P. Schneider*
Schneider Consulting GbR
George-C.-Marshall Ring 33, 61440 Oberursel (Germany)

  DOI: 10.1002/cbic.200400332

conformations were chosen based on existing knowledge among the best-ranked results. Molecule **9** was manually adjusted to fit to the alignment. In molecule **3** the angle between the two planes of the ring systems was set to 90° (Merz, unpublished results). These individual 3D conformations served as query structures for CATS3D similarity searching.

In search for new ligands, we virtually screened the Asinex Gold compound collection (April 2003 version, Asinex Ltd., Moscow, Russia; http://www.asinex.com), which contained 194563 molecules. Counterions were removed by using CLIFF (Molecular Networks GmbH, Erlangen, Germany; http://www.mol-net.de), and, as a prescreening filter, we selected the 20000 most "drug-like" compounds, as described previously.[8a] "Drug-likeness" was calculated from i) the output ("score") of an artificial neural network that was trained to distinguish between "drugs" and "nondrugs",[8] based on topological pharmacophores (CATS approach), ii) predicted aqueous solubility,[11] and iii) calculated polar surface area (PSA) (ASA_P option from MOE). Subsequent principal component analysis of this 3D "drug-likeness" space was performed to obtain uncorrelated variables, and compounds were selected on the basis of their distance to "optimal" variable values (i.e., high drug-likeness score; high solubility value; PSA < 140 Å^2). The result of this procedure can be seen, for example, for the neural network prediction. The average drug-likeness score of the complete Asinex Gold collection according to the artificial neural network was 0.36 ($\sigma = 0.28$), for our screening set the score was 0.60 ($\sigma = 0.23$; higher values indicate more "drug-like" molecules.[8] It should be noted that the selection of the screening compounds resulted from three variables, not just the neural network score. This was done to account for several aspects of the "drug-like" behavior of molecules.[12]

3D conformations of the screening compounds were calculated in MOE by using the MMFF94 force field.[13] The results were restricted to a maximum of the 20 lowest-energy conformations per molecule. Similarity between a database entry and a reference molecule was expressed by the Manhattan distance [Eq. (1)].

$$D_{A,B} = \sum_{i=1}^{i=N} |x_{iA} - x_{iB}| \quad (1)$$

Here A and B indicate the CATS3D vectors of two molecules, x_i is the value of vector element i, and N is the total number of vector elements ($N = 420$). Separate similarity searches were performed with each of the molecules **3**–**9**, and 27 of the top-scoring molecules (Scheme 2) were selected for experimental testing. Molecules were chosen that had low Manhattan distances to one of the reference molecules and that were not too similar to the previously selected molecules, as judged by visual inspection from a medicinal chemistry perspective (Table 1).

To estimate the degree of "scaffold-hopping" we compared the average distance of each molecule **10**–**36** to its respective

Table 1. *Results of virtual screening and the binding assays.*

Molecule no.	Most similar reference molecule	Rank (CATS3D)	Virtual Screening CATS3D Manhattan distance	CATS2D Manhattan distance	MACCS Tanimoto similarity	Binding Assay K_i mGluR5 [μM]	K_i mGluR1 [μM]	Selectivity (K_i mGluR1/ K_i mGluR5)
10	**3**	1	0.68	2.85	0.21	24	> 100	> 4.2
11	**3**	4	0.88	2.2	0.2	> 100	63	< 0.6
12	**3**	5	0.94	5.03	0.17	> 100	41	< 0.4
13	**3**	6	0.95	3.79	0.22	> 100	> 100	1
14	**3**	7	1.02	2.64	0.17	> 100	> 100	1
15	**3**	17	1.12	3.06	0.24	> 100	> 100	1
16	**4**	1	1.52	2.54	0.35	> 100	> 100	1
17	**4**	3	1.67	5.27	0.22	> 100	> 100	1
18	**4**	4	1.67	2.34	0.34	> 100	> 100	1
19	**4**	6	1.73	1.88	0.25	> 100	> 100	1
20	**5**	3	2.14	1.79	0.42	> 100	> 100	1
21	**5**	7	2.22	1.79	0.36	> 100	> 100	1
22	**5**	38	2.52	2.66	0.38	41	64	1.6
23	**6**	5	1.41	2.23	0.48	33	61	1.8
24	**6**	6	1.45	1.91	0.31	12	17	1.5
25	**7**	2	1.55	2.69	0.38	35	> 100	> 2.9
26	**7**	3	1.56	2.41	0.39	> 100	> 100	1
27	**7**	5	1.6	2.62	0.53	> 100	14	< 0.14
28	**8**	2	0.79	5.49	0.38	> 100	> 100	1
29	**8**	7	0.91	5.37	0.24	> 100	> 100	1
30	**8**	9	1	5.37	0.31	40	> 100	2.54
31	**8**	12	1.14	4.81	0.28	> 100	> 100	1
32	**8**	36	1.3	5.33	0.2	14	45	3.2
33	**9**	1	1.49	2.19	0.46	63	> 100	> 1.6
34	**9**	2	1.54	1.94	0.45	38	> 100	> 2.7
35	**9**	5	1.59	2.59	0.46	> 100	> 100	1
36	**9**	7	1.64	6.63	0.46	> 100	> 100	1

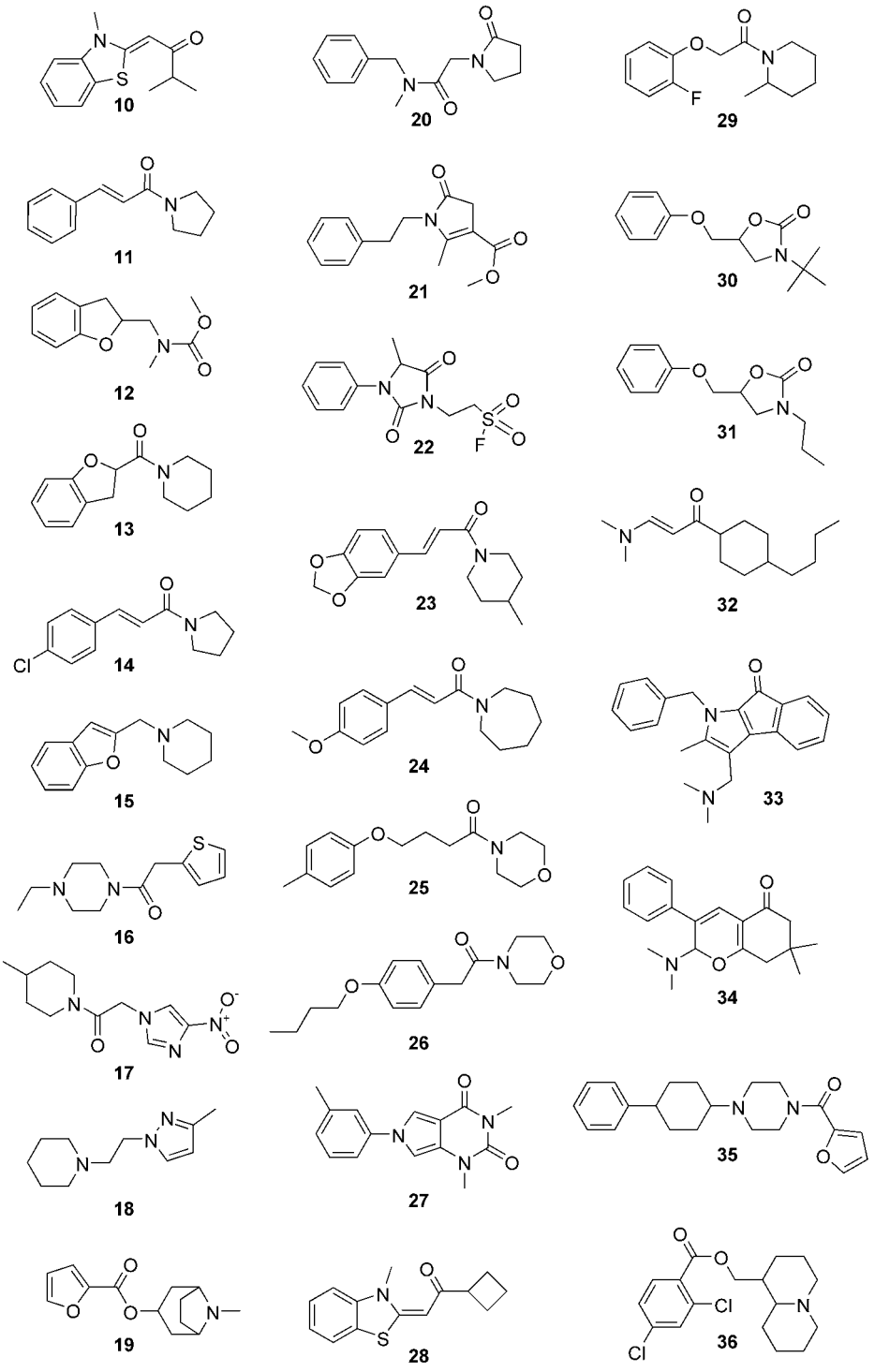

Scheme 2. *Molecules selected by virtual screening.*

nearest reference ($\langle D_{lib}\rangle$) compound with the average distance between the reference molecules **3**–**9** ($\langle D_{ref}\rangle$). Three such indices were employed, the CATS3D Manhattan distance, the topological CATS2D Manhattan distance, and the substructure-based MACCS key Tanimoto similarity from MOE. While the average CATS3D distance of the library compounds to their reference molecules was significantly smaller in comparison to the average distance between the reference molecules ($\langle D_{lib}\rangle = 1.41 \pm 0.45$, $\langle D_{ref}\rangle = 2.66 \pm 0.89$), $\langle D_{lib}\rangle$ was only marginally smaller than $\langle D_{ref}\rangle$ for CATS2D (3.31 ± 1.48 vs. 3.6 ± 1.4). With the MACCS keys, $\langle D_{lib}\rangle$ was smaller than $\langle D_{ref}\rangle$ (0.33 ± 0.11 vs. 0.39 ± 0.15); this indicates a greater similarity among the reference set than between the virtual screening hits and the reference molecules, and demonstrates that the compiled library contains scaffolds that are different from the references (as estimated by MACCS substructure fingerprints) but are still considered isofunctional by the CATS pharmacophore approaches.

In vitro binding studies for mGluR5 were performed on the basis of a [^{3}H]MPEP displacement assay. Estimates of K_i values for the ligands were made from measurements at a fixed concentration of 10 μM. Selectivity of the ligands versus mGluR1, the most similar receptor to mGluR5 within the mGluR family,[1] was assessed by a displacement assay with the Merz proprietary selective mGluR1 antagonist MRZ 3415. Nine molecules (**10**, **22**, **23**, **24**, **25**, **30**, **32**, **33**, **34**) exhibited a K_i value below 70 μM for mGluR5 (Table 1), with structure **10** being the most selective inhibitor. With our assay system, we determined a K_i of 12.5 nM for MPEP on mGluR5.

The predicted rank order of the tested library compounds does not correlate with binding affinity (Table 1). It is evident that the Manhattan distance, which was used for compound prioritization, does not distinguish between molecular attributes that are relevant or irrelevant to a particular receptor–ligand interaction. Furthermore, the small list of virtual hits that was compiled for each reference molecule prevents a sound statistical evaluation.[10,14]

The nine best molecules found were aligned to the reference molecule alignment with the MOE flexible-alignment tool (Figure 2). Compounds **23**, **24**, **25**, and **32** fitted well into the reference alignment (Figure 2a) with the keto group of each molecule superimposed onto the pyridine nitrogen as a hydro-

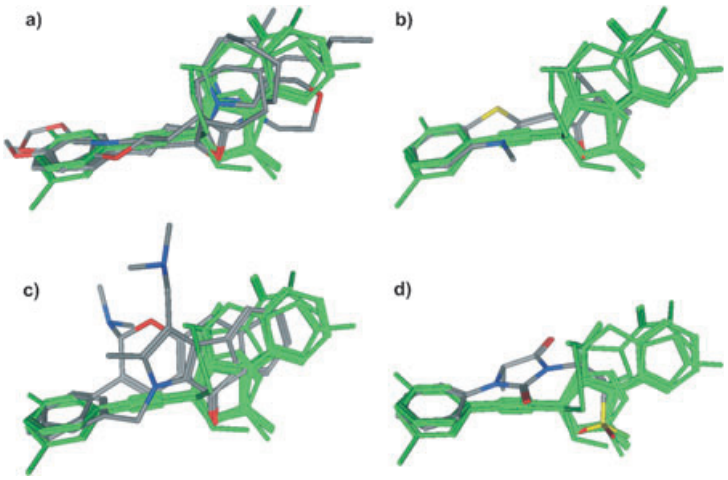

Figure 2. *Flexible alignment of the most potent found mGluR5 modulators to the alignment of reference molecules* ***3****–****9*** *(green). Alignments are shown for a)* ***25****,* ***26****,* ***27****,* ***34****; b)* ***10****; c)* ***35****,* ***36****; d)* ***23****.*

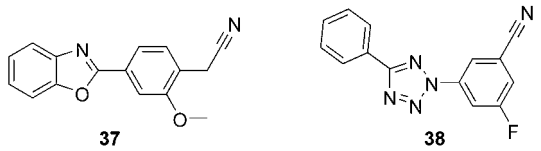

Scheme 3. *Recently reported mGluR5 antagonists with new scaffolds.*

gen-bond acceptor substitute, and the various linker moieties aligned to the triple-bond linkers of the MPEP derivatives. For **30**, a comparable binding mode should be anticipated, but was not found by the flexible alignment since MOE did not recognize the oxazolidine oxygen of **30** as a potential hydrogen-bond acceptor. Based on the alignment, it cannot be decided whether molecules **10**, **33**, **34** and **22** (Figure 2 b–d) were actually aligned in a reasonable fashion. For these molecules, large substructure elements were placed in the MPEP-linker region, which we assume to bind to a narrow part of the receptor-binding pocket. To our surprise **28** and **31**—analogues of ligands **10** and **30**—were shown to be inactive. For both molecules, this effect might be explained by steric restrictions in the receptor.

The selectivity of the hits was low. Compound **27** was even found to be a potent and selective binder of mGluR1. This might indicate the existence of similar binding pockets in both receptor subtypes. Overlap of the binding pockets for antagonists of both receptor subtypes has already been shown.[15] Similar binding pockets are further supported by the weaker mGluR1-selective binder **11**, which is similar to **23**, **24** and **25**, which are more selective toward mGluR5. Compound **14** was inactive in both mGluR1- and mGluR5-binding studies, although it might be regarded as a close analogue of **11**.

A challenging goal of pharmacophore-based similarity searching is "scaffold-hopping".[9] This aim was clearly met by our study. Isofunctional alternatives to the MPEP scaffold were found that provided several starting points for lead-structure development. As an important outcome, the metabolically unstable triple-bond linker present in the MPEP-derived reference molecules is substituted by various alternatives in the compounds that were selected by virtual screening. Note that the double-bond linker of **23**, **24**, and **32** is structurally identical to the one present in SIB-1893 and similar to the linker type of SIB-1757, neither of which was present in the reference collection (Scheme 1). Some of the tested compounds (**12**, **13**, **15**) have structural similarity to the recently reported mGluR5 antagonist **37** (Scheme 3),[17] which was found by HTS. This further underlines the ability of the CATS3D approach to find isofunctional but structurally different scaffolds. Molecule **38**, a recently reported mGluR5 antagonist with a tetrazole linker (Scheme 3),[18] shows that more voluminous groups, as in **22**, might also be allowed in the linker region, assuming a similar binding mode. The novel scaffolds of compounds **33** and **34** present a promising opportunity for straightforward combinatorial design with the aim of significantly improving binding behavior.

One possible reason for the low selectivity of **23**, **24**, **25**, and **32** might be the replacement of the SIB-1893 pyridine by a keto group. While the hydrogen-bond acceptor functionality of the pyridine is maintained, the substitution results in a loss of possible steric and stacking interactions. These findings indicate that the receptor-subtype selectivity of MPEP-like mGluR5 antagonists might be based on steric or π–π stacking interactions mediated by the pyridine ring. Reference molecule **9**, which lacks an aromatic ring, supports the hypothesis that a defined steric interaction in the region of the MPEP pyridine might be sufficient for selectivity.

Summarizing, it has been demonstrated that pharmacophore-based similarity searching can lead to novel, isofunctional molecular scaffolds that provide a basis for lead-structure development. The target was an allosteric binding site of a pharmacologically challenging GPCR.[18] Although homology-based models of the MPEP-binding pocket have been published recently,[15,19] successful virtual screening that exploits this information has not been reported until now. Our entirely ligand-based approach can thus be seen as a working alternative to more-demanding, structure-based design techniques with the main aim of developing novel lead series.

Experimental Section

Materials. [3H]-MPEP was obtained from Tocris Cookson (Bristol, UK). MPEP was synthesized for in-house use as a reference compound according to refs. [4, 20]. Test compounds were purchased as dry powder from ASINEX Ltd. (Moscow, Russia). The ASINEX Gold Collection Database was provided by ASINEX Ltd. [3H]-MRZ 3415 was synthesized by Amersham Biosciences (Buckinghamshire, UK). MRZ 3415 was synthesized for in-house use as a reference compound by the Latvian Institute of Organic Synthesis (Riga, Latvia).

Methods

Membrane preparation. Male Sprague Dawly Rats (approx. 200–250 g) were anaesthetized and decapitated. Forebrains were removed and homogenized (Ultra Turrax, 8 strokes, 600 rpm) in Sucrose (0.32 M). Animals were housed and experiments were performed according to the Animal Rights Commission Allowance #

OR-04 (Hessen, Germany). The suspension was separated in a Centrikon T-2050 Ultracentrifuge (Tegimenta AG, Rotkreuz, Switzerland) at 1500 *g* for 4 min. The supernatant was removed and centrifuged at 20800 *g* for 20 min. The resulting pellet was resuspended in ice-cold distilled water and centrifuged at 7600 *g* for 20 min. Supernatant and loosely associated flocculent membrane material (buffy coat) were removed by gentle trituration of the pellet and centrifuged at 75000 *g* for 20 min. The supernatant was discarded, and the membrane pellet was resuspended by sonication in Tris-Buffer (5 mM, pH 7.4) and afterwards centrifuged at 75000 *g* for 20 min. The last step was repeated twice, and membranes were resuspended in Tris-Buffer (50 mM, pH 7.5).

The concentration of protein was determined by the Lowry protein assay with bovine serum albumin as a standard. Membranes were stored frozen at −24 °C, thawed on the day of the assay, and washed again four times at 75000 *g* for 20 min.

All centrifugation steps were carried out at 4 °C.

[3H]-MPEP binding. After thawing, membranes were washed four times with ice-cold binding buffer containing Tris-HCl (50 mM, pH 7.5). Binding assays were performed at room temperature in duplicate by using fixed concentrations of test compound (10 μM). The assay was incubated for 1 h in the presence of radiotracer (5 nM) and membranes (1.2 mg mL^{-1}), and nonspecific binding was estimated by using MPEP (10 μM). Binding was terminated by rapid filtration through GF 52 glass-fiber filters (Schleicher & Schuell, Dassel, Germany) by using a 1225 Sampling Manifold (Millipore GmbH, Eschborn, Germany). Filters were washed twice with ice-cold assay buffer and transferred to scintillation vials. After addition of Ultima-Gold MV (Packard Bioscience, Groningen, The Netherlands), radioactivity collected on the filters was counted in a 1500 Tri-Carb Packard Scintillation Counter.

[3H]-MRZ 3415 binding. After thawing, membranes were washed four times with ice-cold binding buffer containing Tris-HCl (50 mM, pH 7.5). Binding assays were performed at room temperature in quadruplicate in 96-well format by using fixed concentrations of test compound (10 μM). The assay was incubated for 1 h in the presence of radiotracer (1 nM) and membranes (0.8 mg mL^{-1}), and nonspecific binding was estimated by using MRZ 3415 (10 μM). Directly after transferring the reaction volume into a 96-well multiscreen plate with a 0.22 μm glass fiber filter (Millipore GmbH, Eschborn, Germany), binding was terminated by rapid filtration with a multiscreen vacuum manifold (Millipore GmbH, Eschborn, Germany). Afterwards, filters were washed four times with ice-cold assay-buffer, and Ultima-Gold MV Scintillation Cocktail (Packard Bioscience, Groningen, The Netherlands) was added. After 14–16 h radioactivity was counted in a MicroBeta Trilux (Perkin Elmer Life Sciences GmbH, Rodgau-Jügesheim, Germany).

Solubility determination. Aliquots (40 μL) of the stock-solution (10 mM, dimethyl sulfoxide (DMSO) as solvent) of each test compound were diluted with DMSO (1.96 mL) to a final concentration of 200 μM. 100 μL of this solution were diluted by addition of a solvent consisting of methanol and deionized water (1.99 mL, 1:1). The resulting solution A had a concentration of 10 μM of the test compound containing 5% DMSO. Solution B was prepared in the same manner but with Tris-buffer (50 mM, pH 7.5) as solvent instead of the methanol/deionized water mixture.

To determine peaks of the different solutions, a Hewlett–Packard Series 1100 HPLC device with diode-array detector (Agilent Technologies, Waldbronn, Germany) was used. Both solutions passed separately through a Symmetry C18 Column (Waters Corporation, Milford, MA) with a average pressure of 190 atm. The resulting peaks of both solutions were compared at a wavelength at which the area under the curve (AUC) of the peak of solution A and solution B displayed a maximum. The AUC of solution A was defined as the 100% value. Thus, the solubility of each test compound was determined as follows:

$$\text{Solubility } [\%] = \frac{\text{AUC}_{\text{solution B}}}{\text{AUC}_{\text{solution A}}} \times 100 \quad (2)$$

IC_{50} value estimation. IC_{50} values were estimated from the % of control values from the scintillation assay with a four-parameter logistic equation. If both the radioligand and the competitor reversibly bind to the same binding site, binding at equilibrium follows Equation (3).

$$y = \frac{100\,\%}{1 + (x/\text{IC}_{50})^s} \quad (3)$$

If s is assumed to be 1, Equation (2) can be reformulated to:

$$\text{IC}_{50} = \frac{x}{(100\,\%/y) - 1} \quad (4)$$

where s = slope factor = 1, x = concentration of test compound [μM] in the assay, and y = result of the binding assay for the test compound [% of control]. K_i values were calculated from the IC_{50} values by using the Cheng–Prussof equation.[21]

$$K_i = \frac{\text{IC}_{50}}{1 + (L/K_d)} \quad (5)$$

Here L corresponds to the radioligand concentration, and K_d to its dissociation constant.

Acknowledgement

This research was supported by the Beilstein-Institut zur Förderung der Chemischen Wissenschaften.

Keywords: bioinformatics · drug discovery · G protein-coupled receptors · molecular modeling · pharmacophore

[1] P. J. Conn, J.-P. Pin, *Annu. Rev. Pharmacol. Toxicol.* **1997**, *37*, 205 – 237.
[2] E. Hermans, R. A. Challiss, *Biochem. J.* **2001**, *359*, 465 – 484.
[3] M. Varney, N. D. Cosford, C. Jachec, S. P. Rao, A. I. Sacaan, F. F. Lin, L. Bleicher, E. Santori, P. J. Flor, H. Allgeier, F. Gasparini, R. Kuhn, S. D. Hess, G. Veliçelebi, E. C. Johnson, *J. Pharmacol. Exp. Ther.* **1999**, *290*, 170 – 181.
[4] F. Gasparini, K. Lingenhöhl, N. Stoehr, P. J. Flor, M. Heinrich, I. Vranesic, M. Biollaz, H. Allgeier, R. Heckendorn, S. Urwyler, M. A. Varney, E. C. Johnson, S. D. Hess, S. P. Rao, A. I. Sacaan, E. M. Santori, G. Veliçelebi, R. Kuhn, *Neuropharmacology* **1999**, *38*, 1493 – 1503.
[5] a) **4**: N. D. Cosford, L. Tehrani, J. Roppe, E. Schweiger, N. D. Smith, J. Anderson, L. Bristow, J. Brodkin, X. Jiang, I. McDonald, S. Rao, M. Washburn, M. A. Varney, *J. Med. Chem.* **2003**, *46*, 204 – 206. **5**, **6**, **7**, **8**: V. Mutel, J. U. Peters, J. Wichmann, WO0246166 **2002**; **9**: F. Gasparini, Y. Auberson, S. Ofner, WO03/047581, **2003**; b) D. M. O'Leary, V. Movsesyan, S. Vicini, A. I. Faden, *Br. J. Pharmacol.* **2000**, *131*, 1429 – 1437; c) V. A. Movsesyan, D. M. O'Leary, L. Fan, W. P. Bao, G. Mullins, S. M. Knoblach, A. I. Faden, *J. Pharmacol. Exp. Ther.* **2001**, *296*, 41 – 47.
[6] J. J. Anderson, M. J. Bradbury, D. R. Giracello, D. F. Chapman, G. Holtz, J. Roppe, C. King, N. D. Cosford, M. A. Varney, *Eur. J. Pharmacol.* **2003**, *473*, 1, 35 – 40.
[7] *Virtual Screening for Bioactive Molecules* (Eds.: H.-J. Böhm, G. Schneider), Wiley-VCH, Weinheim, **2000**.

[8] a) G. Schneider, P. Schneider in *Chemogenomics in Drug Discovery* (Eds.: H. Kubinyi, G. Müller), Wiley-VCH, Weinheim, **2004**, pp. 341 – 376; b) E. Byvatov, U. Fechner, J. Sadowski, G. Schneider, *J. Chem. Inf. Comput. Sci.* **2003**, *43*, 1882 – 1889; c) J. Sadowski, H. Kubinyi, *J. Med. Chem.* **1998**, *41*, 3325 – 3329.
[9] G. Schneider, W. Neidhard, T. Giller, G. Schmid, *Angew. Chem.* **1999**, *111*, 3068 – 3070; *Angew. Chem. Int. Ed.* **1999**, *38*, 2894 – 2896.
[10] U. Fechner, L. Franke, S. Renner, P. Schneider, G. Schneider, *J. Comput.-Aided Mol. Des.* **2003**, *17*, 687 – 698.
[11] O. Engkvist, P. Wrede, *J. Chem. Inf. Comput. Sci.* **2002**, *42*, 1247 – 1249.
[12] a) M. S. Lajiness, M. Viet, J. Erickson, *Curr. Opin. Drug Discovery Dev.* **2004**, *7*, 470 – 477; b) W. J. Egan, K. M. Merz, Jr, J. J. Baldwin, *J. Med. Chem.* **2000**, *43*, 3867 – 3877.
[13] T. A. Halgren, *J. Comput. Chem.* **1996**, *17*, 490 – 512.
[14] a) D. Wilton, P. Willett, K. Lawson, G. Mullier, *J. Chem. Inf. Comput. Sci.* **2003**, *43*, 469 – 474; b) J. Hert, P. Willett, D. J. Wilton, P. Acklin, K. Azzaoui, E. Jacoby, A. Schuffenhauer, *J. Chem. Inf. Comput. Sci.* **2004**, *44*, 1177 – 1185; c) M. Whittle, V. J. Gillet, P. Willett, A. Alex, J. Loessel, *J. Chem. Inf. Comput. Sci.* **2004**, *44*, 1840 – 1848.
[15] A. Pagano, D. Ruegg, S. Litschig, N. Stoehr, C. Stierlin, M. Heinrich, P. Floersheim, L. Prezeau, F. Carroll, J. P. Pin, A. Cambria, I. Vranesic, P. J. Flor, F. Gasparini, R. Kuhn, *J. Biol. Chem.* **2000**, *275*, 33 750 – 33 758.
[16] B. Wang, J. M. Vernier, S. Rao, J. Chung, J. J. Anderson, J. D. Brodkin, X. Jiang, M. F. Gardner, X. Yang, B. Munoz, *Bioorg. Med. Chem.* **2004**, *12*, 17 – 21.
[17] J. Roppe, N. D. Smith, D. Huang, L. Tehrani, B. Wang, J. Anderson, J. Brodkin, J. Chung, X. Jiang, C. King, B. Munoz, M. A. Varney, P. Prasit, N. D. Cosford, *J. Med. Chem.* **2004**, *47*, 4645 – 4648.
[18] a) S. Rees, D. Morrow, T. Kenakin, *Recept. Channels* **2002**, *8*, 261 – 268; b) L. T. May, A. Christopoulos, *Curr. Opin. Pharmacol.* **2003**, *3*, 551 – 556.
[19] P. Malherbe, N. Kratochwil, M. T. Zenner, J. Piussi, C. Diener, C. Kratzeisen, C. Fischer, R. H. Porter, *Mol. Pharmacol.* **2003**, *64*, 823 – 832.
[20] H. Sashida, M. Kato, T. Tsuchiya, *Chem. Pharm. Bull.* **1988**, *36*, 3826 – 3832.
[21] Y. Cheng, W. H. Prusoff, *Biochem. Pharmacol.* **1973**, *22*, 3099 – 3108.

Received: September 15, 2004
Published online on March 2, 2005

